Springer

KSME

Journal of Mechanical Science and Technology 24 (2010) 343~350
www.springerlink.com/content/1738-494x
DOI 10.1007/s12206-009-1108-7

Novel design of a small field robot with multi-active crawlers capable of autonomous stair climbing †

Byeong-Sang Kim[1], Quy-Hung Vu[1], Jae-Bok Song[1,*] and Chung-Hyuk Yim[2]

[1]*School of Mechanical Engineering, Korea University, Seoul, 136-713, Korea*
[2]*School of Mechanical Design & Automation Engineering, Seoul National University of Technology, Seoul, 139-743, Korea*

(Manuscript Received February 23, 2009; Revised September 18, 2009; Accepted October 6, 2009)

Abstract

Mobile robots often encounter complex obstacles during their operation, not the least of which are stairs. Suitable mechanical structures and adequate control algorithms are both equally important in stair climbing. This paper proposes a novel design for a multi-active crawler robot (MACbot) capable of autonomous stair climbing. The MACbot has four track modules for extended mobility and a recovery arm that facilitates self-rescue capabilities. By adopting the proposed smart clutch mechanism, the MACbot can provide a variety of motions with a minimum number of motors. This paper presents a static analysis for the mechanical design and details the stability analysis for an autonomous stair climbing algorithm. A series of experiments show that the MACbot can autonomously climb stairs reasonably well.

Keywords: Autonomous stair climbing; Clutch mechanism; Tracked robot; Stability analysis

1. Introduction

Tracked robots are used for reconnaissance in dangerous areas such as at the scene of a fire or a crime. In such situations, they are operated by remote control based on the visual information transmitted from a camera mounted on the robot. However, remote operation is very difficult when a robot encounters complex obstacles such as stairs because the information provided by vision and range sensors is not intuitive enough to control the robot. To cope with these problems, both suitable mechanical structures and adequate control algorithms are equally important in successfully climbing stairs.

In the mobile robotics field, various research efforts have been directed toward indoor and outdoor navigation using the sensor fusion [1, 2] and the development of a robot capable of stair climbing [3-8]. For example, a double-track mobile robot, composed of the front and rear bodies with tracks and the passive joint, was developed to provide a high mobility and good ground adaptability [3]. A tracked mobile robot based on a linkage mechanism actuator (LMA), composed of two parallel arms to control the shape of the tracks, was developed to autonomously climb and descend stairs [4]. A new driving mechanism capable of transforming the geometry of the track was proposed to climb the stairs [5]. Another example involves a tracked robot that can climb the stairs autonomously by using a vision sensor, a 3-axial gyroscope and a Kalman filter in attitude estimation [6]. However, most of them had a relatively large size for stair climbing, which led to the difficulty in working in the narrow area.

To cope with these problems, the multi-active crawler robot (MACbot) proposed in this paper was focused on the small-size, lightweight, high practicality and high capability of stair climbing. The MACbot has four track modules that have the dual functions of the tread drive and the track module drive. The clutch mechanism enables the MACbot to switch the path of power transmissions associated with the tread and track module. When the MACbot is in rugged terrain in tread drive mode, the track modules can freely rotate around their pivots so as to provide stable contact between the tracks and the ground. With five motors, four located on each track and one in the robot body, the MACbot can operate by running four tracks simultaneously and rotating them as necessary. In addition, the MACbot can overcome a relatively high obstacle for its size. Compared with the previous track robots, the MACbot is small and lightweight but it still works well on the normal stairs.

The premier features of the MACbot can be summarized in following three main points: multiple functions with a minimal number of motors, self-rescue capabilities and autonomous stair climbing ability. From a practical point of view, the number of motors is a very important consideration since it

† This paper was recommended for publication in revised form by Associate Editor Doo Yong Lee
*Corresponding author. Tel.: +82 2 3290 3363, Fax.: +82 2 3290 3757
E-mail address: jbsong@korea.ac.kr

directly relates to the cost of the robot. By adopting a smart clutch mechanism, the MACbot still provides a variety of functions such as the traveling, climbing and recovering with a minimal number of motors. When the MACbot is flipped upside down, the recovery arm helps it to reposition itself right-side-up and the robot can continue to perform its mission without any human intervention. Furthermore, the MACbot can climb stairs autonomously by using information about the robot's posture and obstacles.

The remainder of this paper is organized as follows: Section 2 describes the concept and mechanical structure of the MACbot. Section 3 presents the static analysis for the mechanical design. Section 4 details the stability analysis for the autonomous stair climbing algorithm. The autonomous stair climbing strategy and the experimental results are shown in Section 5. Finally, Section 6 presents the conclusions.

2. Multi-active crawler robot

2.1 Concept of MACbot

As shown in Fig. 1, the MACbot is comprised of four active track modules, three clutches and the recovery arm. The two front track modules including the clutches can go forward by crawling with the treads and rotating them around their pivots as necessary. The other clutch placed at the robot body enables the MACbot to transmit the power of the recovery motor to the recovery arm and rear track modules, connected to the same power transmission. Unlike the front track modules, the rear track modules can go both forward and backward.

The MACbot provides three drive modes: the normal mode for regular terrain (Fig. 2(a)); the obstacle mode for rough terrain (Fig. 2(b)); and the recovery mode (Fig. 2(c)). When the MACbot encounters a high step that it cannot negotiate in the normal mode, it activates the obstacle mode as shown in Fig. 2. When the two front tracks reach the obstacle (Fig. 2(a)), it starts to rotate to climb it (Fig. 2(b)). After the two front tracks are successfully positioned on the obstacle or step, the two rear tracks approach then climb up onto the step. When the MACbot is flipped upside down, the recovery arm can help it to reposition itself right-side-up (Fig. 2(c)).

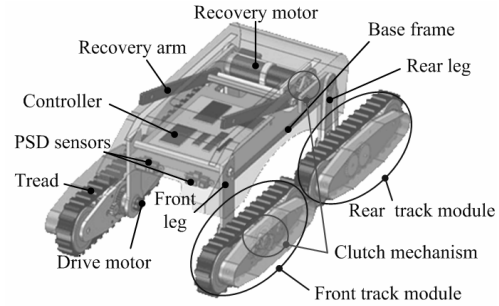

Fig. 1. 3D model of MACbot.

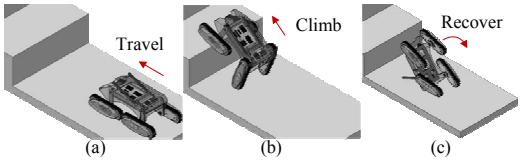

Fig. 2. Three drive modes: (a) normal mode, (b) obstacle mode, and (c) recovery mode.

2.2 Clutch mechanism

The clutch mechanism shown in Fig. 3 switches the driving modes according to certain conditions. This mechanism was proposed in order to limit power consumption and minimize the number of motors necessary for operation. As shown in Fig. 3(a), the clutch mechanism based on a planetary gear system is composed of a sun gear, a planet gear, a carrier and a torsion spring. Without the internal ring gear used in general planetary trains, a small friction force generated by the spring is required to prevent free motion from occurring between the sun gear and the carrier. In Fig. 3(a), the clutch mechanism is in a neutral position, so no engagement occurs and gear 1 and gear 2 are idle. When the sun gear rotates counterclockwise (CCW), the planet gear approaches gear 1, as shown in Fig. 3(b). In the same manner, if the sun gear rotates clockwise (CW), the planet gear now meshes with gear 2 as shown in Fig. 3(c). With this clutch mechanism, two drive modes can be obtained by using a single motor, and the function depends on the rotational direction of the motor. This type of clutch mechanism is used in the two front track modules and in the recovery mechanism.

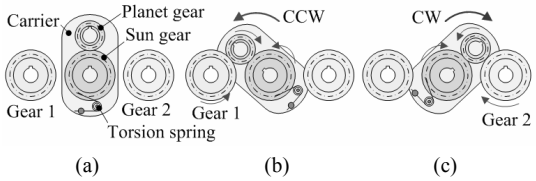

Fig. 3. Clutch mechanism based on a planetary gear system: (a) neutral state, (b) mesh with gear 1, and (c) mesh with gear 2.

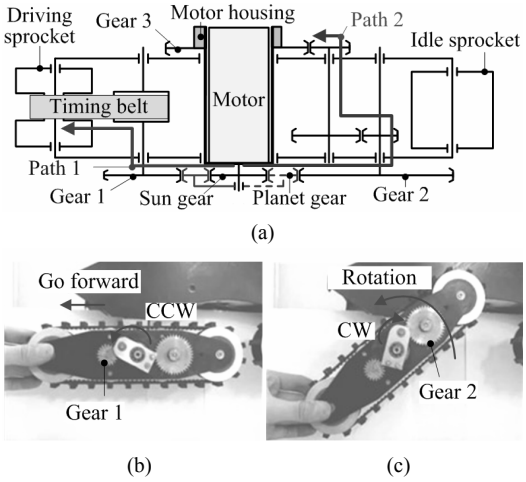

Fig. 4. Front track module: (a) gear diagram, (b) normal mode, and (c) obstacle mode.

2.3 Mechanical design

With the clutch mechanism, the front track can be driven and rotated with a single motor. There are two paths to transmit the torque generated by the motor as shown in Fig. 4(a). The track module can rotate around the motor housing connected to the robot body through the bearing. When the motor rotates CCW, the normal mode is activated and the planet gear engages with gear 1. As a result, the motor torque is transmitted to the driving sprocket (gear ratio of 1.7:1) through path 1. The belt connecting the driving sprocket to the idle sprockets rotates CCW so the track module can go forward as shown in Fig. 4(b).

When the robot encounters an obstacle, the rotational direction of the motor is changed to the CW direction and the planet gear then meshes with gear 2. The torque transmitted to gear 3, which is connected to the motor housing via path 2, has a gear ratio of 7.6:1. Since the motor housing is connected to the front leg, the track module rotates CCW relative to the robot body as shown in Fig. 4(c). The obstacle mode needs a higher torque than the normal mode, so the gear ratio is 4.5 times higher than that of the normal mode.

Compared to the front track module, the structure of the rear track is simple. Instead of moving ahead and rotating itself, it can move either forward or backward. However, the rear track module must rotate itself when the MACbot is operated in the obstacle mode. The recovery motor and clutch mechanism helps to do that as illustrated in Fig. 5. During obstacle mode, the torque of the recovery motor is transmitted to the rear track module through the timing belt/pulley connected to the rear track module as shown in Fig. 5(b). In addition, the recovery motor is used to rotate the recovery arm and push on the ground and recover its pose when the MACbot is flipped upside-down as shown in Fig. 5(c).

Most robots overcome an obstacle with forward movement, and backward movement is required to change the desired path when they encounter a corner. Replacing the function of going backward of the front tracks with the function of their rotation, the MACbot can easily overcome relatively high obstacles for its size, while the number of the motors is maintained. The MACbot goes backward with the rear track modules by pulling the front track modules, because the clutches allow the treads of the front tracks to crawl freely.

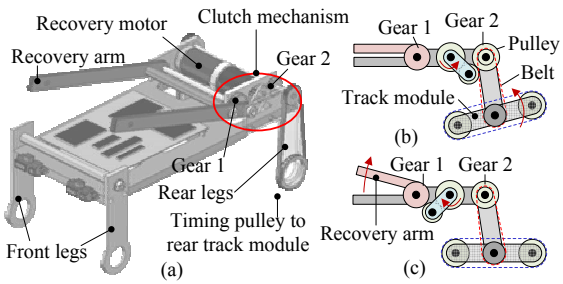

Fig. 5. Body design: (a) mechanical structure of body, (b) obstacle mode, and (c) recovery mode.

2.4 Prototype of MACbot

The fabricated MACbot capable of overcoming high obstacles is shown in Fig. 6 and its specifications are listed in Table 1. The robot uses five BLDC motors equipped with speed reducers and encoders. Two microcontroller processor units (ATMega 128) with small motor driver ICs are used to control the motors. To measure the distance between the robot and the obstacle, two PSD sensors (GP2D120XJ00F) are mounted at the front of the robot body. Three optical encoders are used to provide the rotation angle of the four tracks around their pivots. The 3-axis accelerometer (A7260 K638051) is also integrated to measure the inclination angle of the body and the direction of gravity. Considering the ratio of the height of the stair (15 cm) to the height of the robot (17 cm) is 0.88, the MACbot can overcome a relatively high obstacle for its size.

3. Static analysis

3.1 Obstacle mode

It is very difficult for a small robot to overcome obstacles such as stairs in the normal mode because there is not sufficient friction between the tread and the ground. To cope with this problem the robot switches from normal mode to obstacle mode as shown in Fig. 7(a). The front track module simultaneously contacts the rising edge (contact point A) and the ground (contact point B) at the corner. The rear track module contributes a force f_2 that pushes the front track module toward the rising edge to increase the frictional force F_e. The required torque to climb an obstacle can be calculated by applying the force and moment balance equations.

At the rising edge, the front track module is subject to the total reaction force F_e. Thus, the force balance equation in the x direction can be obtained by

Table 1. Specifications of MACbot.

Parameters	MACbot
Size	27x49x17 cm
Total weight	4.1 kg
Max. height of obstacle	18 cm
Speed in normal mode	0.5 m/s
Speed in obstacle mode	0.2 m/s
Ability in stair climbing	15cm in height 30cm in depth

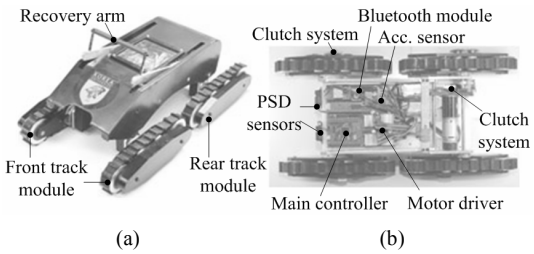

Fig. 6. MACbot: (a) prototype, and (b) internal parts.

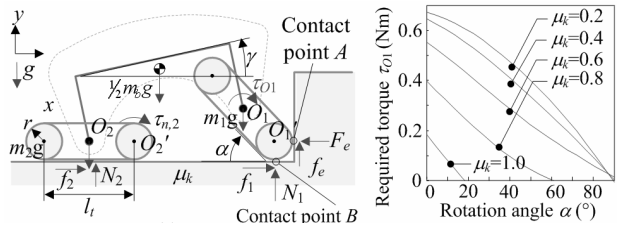

Fig. 7. Static analysis: (a) schematic diagram, and (b) required torque of front track for different friction coefficient.

$$F_e = f_e / \mu_k = (N_1 + N_2)\mu_k \tag{1}$$

where μ_k is the coefficient of kinetic friction, f_e is the frictional force of the front track at the contact point A, and N_1 and N_2 are the normal forces on the front and rear tracks, respectively.

As the front track rotates, the robot body inclines so the distributed mass of the body m_{b1} and m_{b2} at the two points O_1, O_2 changes as follows:

$$\begin{aligned} m_{b1} &= \frac{d_b \cos\gamma - h_b \sin\gamma}{2l_b \cos\gamma} m_b \\ m_{b2} &= \frac{l_b \cos\gamma - (d_b \cos\gamma - h_b \sin\gamma)}{2l_b \cos\gamma} m_b \end{aligned} \tag{2}$$

where d_b (= 11 cm) and h_b (= 10 cm) are the distance and height to the mass center, l_b (= 21 cm), m_b (= 2.1 kg) and γ are the length, the mass and the inclination angle of the robot body, respectively. From the moment balance at point O_2, N_1 can be given by

$$\begin{aligned} N_1 = {} & \frac{(m_1 + m_{b1})gl_b \cos\gamma - (m_{b2} + m_2)g\mu_k^2 (l_b \cos\gamma + \frac{l_t \cos\alpha}{2} + r)}{\mu_k r + \mu_k^2 (l_b \cos\gamma + \frac{l_t \cos\alpha}{2} + r) + (l_b \cos\gamma + \frac{l_t \cos\alpha}{2})} \\ & - \frac{r(m_2 + m_{b2})g\mu_k}{\mu_k r + \mu_k^2 (l_b \cos\gamma + \frac{l_t \cos\alpha}{2} + r) + (l_b \cos\gamma + \frac{l_t \cos\alpha}{2})} \end{aligned} \tag{3}$$

where r (= 3 cm) is the radius of the driving sprocket, l_t (= 18 cm) is the length of the track and α is the rotation angle of the front track, respectively. Substituting Eq. (1) and (3) into Eq. (4) yields the required torque τ_{O1} to overcome the obstacle as shown in the following equation:

$$\begin{aligned} \tau_{O1} = {} & (r + \frac{l_t \sin\alpha}{2}) f_1 + (r + \frac{l_t \cos\alpha}{2}) f_e \\ & + \frac{l_t \cos\alpha}{2} N_1 - \frac{l_t \sin\alpha}{2} F_e \end{aligned} \tag{4}$$

The torque τ_{O1} required for the front track as a function of α varies depending on the different values of μ_k as shown in Fig. 7(b). For common conditions, the maximum torque (= 0.55 Nm) occurs at the start of the front track rotation if the friction coefficient is 0.6 (normal condition for a tracked vehicle). The maximum torque of the robot must be much higher than the computed torque since factors such as internal friction were neglected in the computation. In the actual system, each track module consisted of a 5W BLDC motor that provided a maximum torque of about 1.7 Nm and 7.6 Nm for the normal mode and obstacle mode, respectively. Fig. 8 shows that the torque is enough to lift the robot body up in order to climb a step.

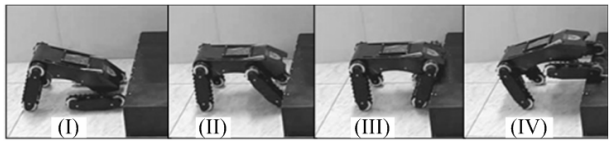

Fig. 8. Sequence of robot motion in the obstacle mode.

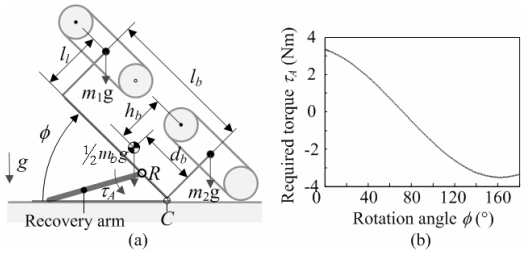

Fig. 9. Recovery mode: (a) schematic diagram, and (b) torque response as a function of rotation angle.

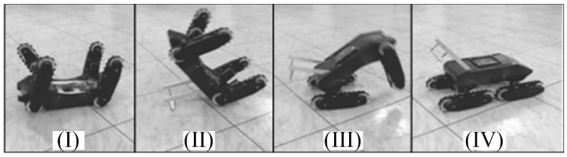

Fig. 10. Sequence of recovery mode.

3.2 Recovery mode

When the robot is overturned and no track is in contact with the ground, the robot must reposition itself on its tracks. The recovery motor rotates the recovery arm CCW as illustrated in Fig. 9(a). From the moment balance at point C, the required torque at point R can be described by the following:

$$\begin{aligned} \tau_R > {} & m_1 g(l_b.\cos\phi - l_l \sin\phi) - m_2 l_l \sin\phi \\ & + \tfrac{1}{2} m_b g\left[d_b.\cos\phi - (l_l - h_b)\sin\phi\right] \end{aligned} \tag{5}$$

where l_b (= 21cm) is the body length, l_l (= 10 cm) is the leg length, and ϕ is the rotation angle of the recovery arm. Fig. 9(b) shows the torque required to turn the robot body as a function of ϕ. The maximum required torque is 3.2Nm.

In the actual system the torque of the recovery motor was chosen as 3.75 Nm. As shown in Fig. 10, the MACbot can stand by itself when it is overturned.

4. Stability analysis

When the MACbot encounters stairs, it changes its operation mode from normal to obstacle mode as explained in Section 2.1. During this mode the contact configuration between

the tracks and the ground changes and sometimes the robot can roll over. Therefore, a safe working area must be considered for all changes in the climbing motion. The center of mass (CM) of the MACbot is constantly changing and the position of the CM depends on both the track angles (α and β) and the body angle (γ). By using the feedback information from the optical and acceleration sensors, all states of the robot can be described in real time. To conduct stable stair climbing, two criteria are required: the stability of CM and the moment balance during stair climbing as shown in Fig. 11. CF and CR mean the center of the front and rear track modules, respectively.

4.1 Stability of center of mass

The robot configuration related to the geometry of the stairs is continuously calculated throughout the climbing process until the robot completes its operation. For the stability analysis shown in Fig. 12 (a), three types of information are used: the rotating angles of the tracks; the distance from the robot to the rising step edge; and the inclination angle of the body. The CM can be obtained through the following relationship:

$$\begin{aligned} x_{cm} &= x_{O2} + d_{cm}\cos\gamma - h_{cm}\sin\gamma \\ y_{cm} &= y_{O2} + d_{cm}\sin\gamma + h_{cm}\cos\gamma \end{aligned} \tag{6}$$

where x_{O2} and y_{O2} are the location of the CM of the rear track, d_{cm} (= 10 cm) and h_{cm} (= 3 cm) are the distance to and height of the CM of the robot, respectively. To maintain the stable motion, x_{cm} must be placed between the contact positions of the front track (x_{C1}) and the rear track (x_{C2}).

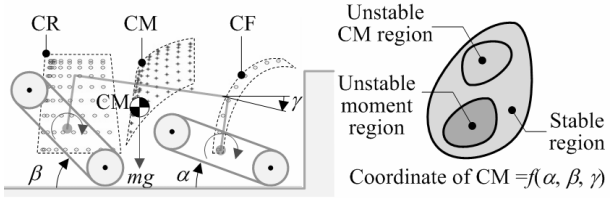

Fig. 11. Stability criteria: (a) possible locations of CF, CM and CR, and (b) diagram for stable region.

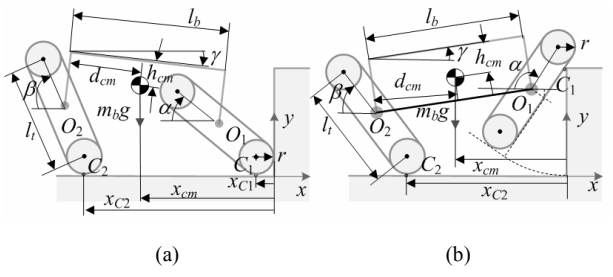

Fig. 12. Schematic for geometry calculation for stair climbing: (a) rotation process, and (b) lifting process.

In the next state (Fig. 12(b)), the robot starts to ride on the stair edge. With the same approach stated above, the position of the CM can be determined and the height of the obstacle can be estimated by

$$\begin{aligned} h_o &= \frac{y_{O1} + r\cos\alpha - (\frac{l_t+2r}{2})\sin\alpha}{1-\sin\alpha} \\ y_{O1} &= r + \frac{l_t}{2}\sin\beta + l_b\tan\gamma \end{aligned} \tag{7}$$

where y_{O1} is the y coordinate of the CM of the front track, r is the track radius, and l_t is the track length, l_b is the length of the robot body. α, β and γ are the angles of the front track, the rear track, and the robot body. α should be larger than 90° and smaller than 180° (90° $< \alpha \leq$ 180°) because (7) is derived from the geometric analysis when the front tracks stand on the upper step. After the front track fully stands on the upper step, the rear track approaches and rides on the step edge to complete the climbing process of the first step.

The CM can be fully managed and is determined to be in either the stable region or the unstable region. By conducting all geometric calculations for the complete stair climbing process, all locations of the robot's CM are obtained as shown in Fig. 13. The operation of the robot must stop at the unstable region. As the obstacle height decreases, the unstable region also decreases. According to the analysis, the unstable region starts to disappear when the obstacle height is 13cm, which means that no danger of unstable motion exists for the robot operation.

4.2 Moment balance

After the front track of the MACbot is placed on the upper step, the motor installed at the rear track applies the torque τ_{O2} to rotate the rear track. The reactive torque is then exerted on the body at the point O_2 as shown in Fig. 14.

As the obstacle height increases, the anti-rollover torque τ_a contributed by the body weight and front track decreases. As the distance between the CM of the body and the point O_2 gets shorter, the robot becomes more likely to roll over. The torques τ_a and τ_{O2} are given by

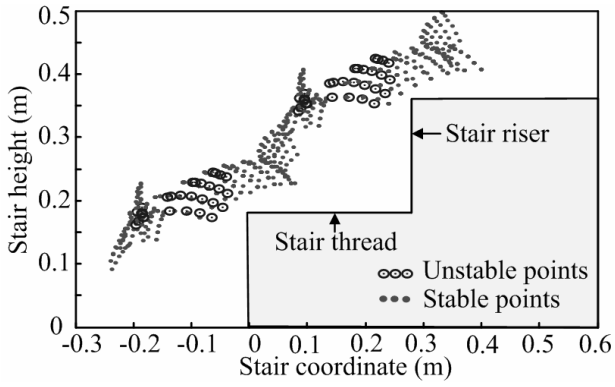

Fig. 13. Locations of the CM of the MACbot.

$$\tau_a = (m_1 + m_{b1}) g l_b \cos\gamma \quad (8)$$

$$\tau_{O2} = (m_2 + m_{b2}) g l_t / 2 \quad (9)$$

where m_1 (= 0.5 kg) and m_2 (= 0.45 kg) are the mass of the front and rear tracks, and m_{b1} and m_{b2} are the distributed mass of the robot body at the front and rear tracks, respectively.

To prevent rollover, τ_a must be larger than τ_{O2}. When the inclination angle of the body γ increases from zero to 90°, the behavior of τ_a and τ_{O2} varies as shown in Fig. 15. If γ is smaller than a critical value of γ_C or the obstacle height is smaller than a certain value h_{limit}, the robot can avoid rollover. The maximum value of h_{limit} is 13cm and it can be obtained by

$$h_{\text{limit}} = l_b \sin\gamma_C \quad (10)$$

where l_b = 21cm and γ_C = 43°. From the analysis explained above, the obstacle can be classified into two cases: the *low obstacle* whose height is lower than 13 cm and the *high obstacle* whose height is higher than 13 cm. The rollover problem never occurs for a low obstacle.

5. Autonomous stair climbing

The MACbot can climb stairs autonomously by executing the proposed scheme based on information provided by the sensors. Furthermore, a stability analysis is incorporated into the autonomous stair climbing algorithm to guarantee the stable motion of the robot. It is very important to know the geometric information of the stair because this directly affects the success of stair climbing.

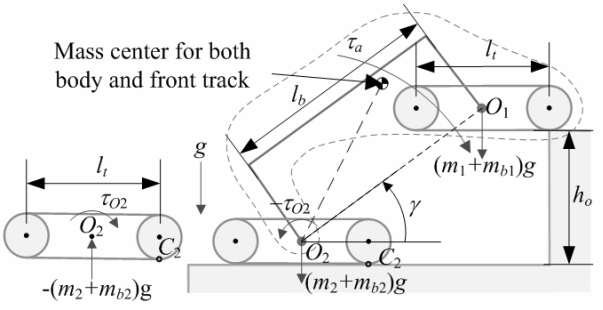

Fig. 14. Free body diagram for MACbot.

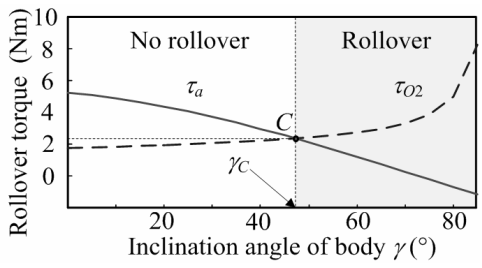

Fig. 15. Moment condition for anti-rollover.

Fig. 16 shows the sequence of robot motions. At the beginning the robot moves close to the stair. The PSD sensor continuously provides the distance between the robot and the stair. When the distance to the step riser becomes smaller than 60 cm, the rear tracks rotate 110° to avoid the unbalanced moment condition as shown in Fig. 16(a). At the next step, when the distance is smaller than half of the track length, the front tracks rotate 200° to ride on the upper step as shown in Fig. 16(b) and (c). At a 90° front track angle (Fig. 16(b)), the step depth d_s can be obtained as the difference between the distance d measured by the PSD sensor and the track radius r.

When the front tracks fully stand on the upper step, the step height can be estimated by Eq. (7). After placing itself on the upper step, the robot moves a distance of d_x before the rear tracks start rotating to ride on the upper step as shown in Fig. 16(c) and (d). The inclination angle of the robot body γ should be smaller than γ_C (= 43°) throughout all stages in order to avoid rollover. Furthermore, the rotation angle of the front and rear tracks must be controlled to guarantee that the distance between the two contact points C_1 and C_2 is shorter than the stair depth d_s. If d_s is shorter than the distance between C_1 and C_2, then the control algorithm is slightly modified to adapt the stairs because the rear tracks cannot stand on the same step on which the front tracks stand. Then, as shown in Fig. 16(e), the rear and front tracks simultaneously rotate until the front tracks fully ride on the upper step. After this step a new sequence of operations are repeated from stage 2 as described in Fig. 16(f). Without any obstacles within 30 cm, the MACbot switches the obstacle mode to the normal mode. All opera-

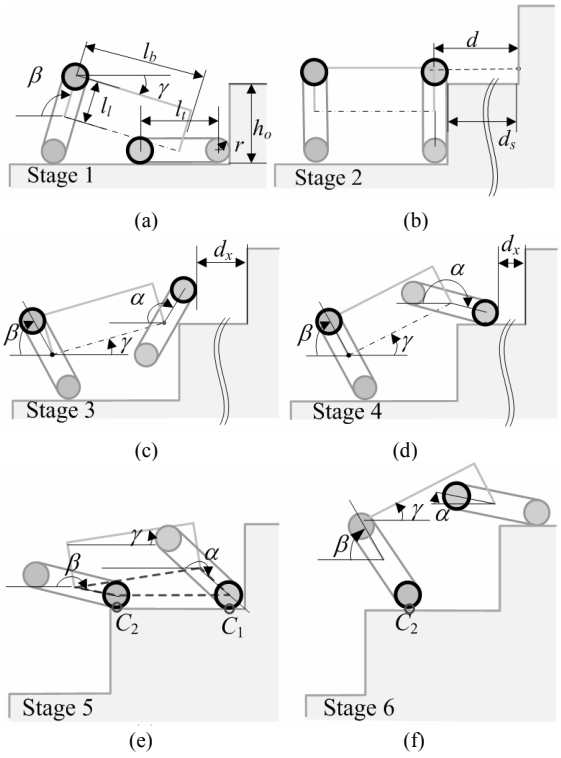

Fig. 16. Sequence of autonomous stair climbing movements.

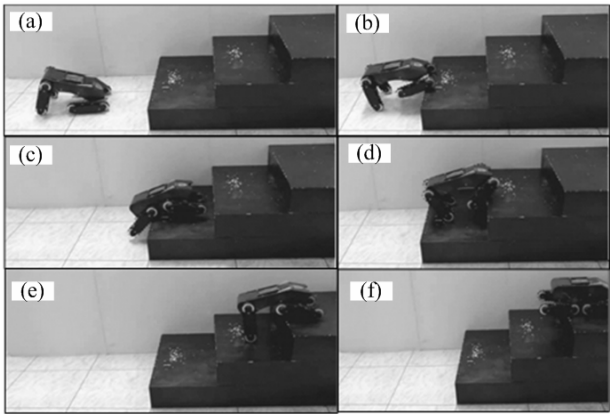

Fig. 17. Autonomous stair climbing.

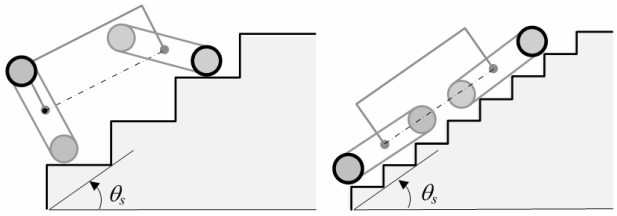

Fig. 18. Different shapes of stairs: (a) medium-size stair, and (b) small-size stair.

tions will be halted if the stability condition is not met.

To verify the performance of the stair climbing algorithm of the MACbot, various experiments were conducted for autonomous stair climbing. The size of the stairs used in this experiment was 15cm by 30cm by 50cm for the height, depth and width, respectively. Fig. 7 shows the sequence of movements for autonomous stair climbing. The experimental results demonstrate that the MACbot can climb stairs reasonably well.

The MACbot can climb the stairs in different ways for a different size, as shown in Fig. 18. For example, if the MACbot climbs the medium-size stairs as shown in Fig. 18(a), the stair climbing strategy is similar to the previous case, but the rear tracks are placed two steps lower than the upper step on which the front tracks stand. On the other hand, if the MACbot climbs the small-size stairs as shown in Fig. 18(b), the MACbot can climb it using the normal mode.

6. Conclusion

In this research, a multi-active crawler robot was proposed and an autonomous stair climbing algorithm was successfully implemented. The stability algorithm for stair climbing always ensures that the center of mass of the MACbot will be placed in the stable region. This algorithm greatly improves the controllability of the MACbot, which reduces the burden of the operator to control the robot for stair climbing. From this research the following conclusions were drawn.

(1) The MACbot can travel with four driving tracks, and sometimes these tracks can be rotated to overcome obstacles.
(2) By using a clutch based on a planetary gear system, the MACbot provides three different modes: normal mode, obstacle mode and recovery mode.
(3) When it is flipped upside-down, the recovery arm can help it to reposition the robot right-side-up and it can continue to perform its mission without human intervention.
(4) Considering the ratio of robot height to obstacle height, the MACbot can overcome a relatively high obstacle for its size.
(5) The MACbot can accomplish complicated tasks such as autonomous stair climbing.

The robot is able to travel over a vast variety of outdoor and indoor terrains. In certain catastrophes, such as landslide, earthquake or building collapse, the robot can be used to rescue or search for missing persons.

Acknowledgment

This work was partly performed for the project “Development of Security Robots” and supported by the Center for Autonomous Intelligent Manipulation under Human Resources Development Program for Convergence Robot Specialists (Ministry of Knowledge Economy).

References

[1] Y. J. Lee, B. D. Yim and J. B. Song, Mobile robot localization based on effective combination of vision and range sensors, *International Journal of Control, Automation, and Systems*, 7 (1) (2009) 97-104.
[2] J. Laneurit, R. Chapuis and F. Chausse, Accurate vehicle positioning on a numerical map, *International Journal of Control, Automation, and Systems*, 3 (1) (2005) 15-31.
[3] C. H. Lee, S. H. Kim, S. C. Kang, M. S. Kim and Y. K. Kwak, Double-track mobile robot for hazardous environment, *Advanced Robotics*, 17 (5) (2003) 447-459.
[4] P. Ben-Tzvi, S. Ito and A. A. Goldenberg. Autonomous stair climbing with reconfigurable tracked mobile robot, *IEEE International Workshop on Robotic and Sensors Environments*, (2007) 1-6.
[5] S. K. Lim, D. I. Park and Y. K. Kwak, A new driving mechanism to allow a rescue robot to climb stairs, *International Journal of Precision Engineering and Manufacturing*, 8 (3) (2007) 3-7.
[6] A. I. Mourikis, N. Trawny, S. I. Roumeliotis, D. M. Helmick and L. Matthies, Autonomous stair climbing for tracked vehicles, *International Journal of Robotics Research & International Journal of Computer Vision - Joint Special Issue on Vision and Robotics*, 26 (7) (2007) 737- 758.
[7] H. Schempf, AURORA-minimalist design for tracked locomotion, *Robotics Research*, 6 (2001) 453-465.
[8] G. Lan, S. Ma, K. Inoue and Y. Hamamatsu, Development of a novel crawler mechanism with polymorphic locomotion,

Advanced Robotics, 21 (3) (2007) 421-440.

Byeong-Sang Kim received the B.S. in Mechanical Engineering from Korea University in 2004. He is currently a Ph.D. candidate at the School of Mechanical Engineering, Korea University. His research interests include design and control of variable stiffness actuator, robot manipulator and mobile robot.

Vu-Quy Hung received the B.S. degree from Hanoi University of Technology in 2004 and the M.S. in Mechanical Engineering from Korea University in 2008. His research interests include variable stiffness actuator, mobile robotics and bio-inspired robotics.

Jae-Bok Song received the B.S. and M.S. in Mechanical Engineering from Seoul National University in 1983 and 1985, respectively, and the Ph. D. in Mechanical Engineering from MIT in 1992. He joined the faculty of the School of Mechanical Engineering, Korea University in 1993. Currently, he is a director of Intelligent Robotics Research Center at Korea University. He is also an editor for the International Journal of Control, Automation and Systems. His current research interests include safe manipulators, design and control of robotic systems, and mobile robot navigation.

Chung-Hyuk Yim received the B.S., M.S. and Ph. D in Control and Instrumentation from Seoul National University, Korea in 1987, 1989, and 1994, respectively. He was a senior researcher at Samsung Electronics for 1994 - 1997. He is currently a professor at the School of Mechanical Design and Automation Engineering at Seoul National University of Technology. His research interests include motion control.